Interocular correlation sensitivity and its relationship with stereopsis

Alexandre Reynaud

McGill Vision Research, Department of Ophthalmology, McGill University, Montreal, Canada

Robert F. Hess

McGill Vision Research, Department of Ophthalmology, McGill University, Montreal, Canada

Stereoscopic vision uses the disparity between the images received by the two eyes to derive three-dimensional estimates. Here, we were interested in providing a measure of the strength of binocular vision alternate to disparity processing. In particular, we wanted to assess the spatial dependence of sensitivity to detect interocular correlation (IOC). Thus we designed dichoptic stimuli composed of bandpass textures whose IOC is sinusoidally modulated at different correlation frequencies and compared sensitivity to these stimuli to that of analogous stimuli modulated in disparity. We observed that the IOC sensitivity is low pass/band pass and increases with stimulus duration and contrast in a similar way to that of disparity sensitivity. IOC sensitivity is only weakly, though significantly, correlated with disparity sensitivity in the population. It could provide an alternate measure of binocular sensitivity.

Introduction

We benefit greatly from having two frontally placed eyes with a wide binocular overlap in the field of view. The brain has a duplicated view of everything in the world, albeit from a slight displacement of around 6 cm, the interpupillary distance. This results in not only a strong correlated signal from the two eyes but also the ability to use any slight difference in the spatial distribution of the signals between the two eyes to derive three-dimensional (3D) estimates. This computation could be mediated by on and off channels subserving image similarities and differences between the two eyes (Kingdom, 2012; Li & Atick, 1994; May, Zhaoping, & Hibbard, 2012). For a given disparity, the degree of correlation in the signals between the two eyes provides, in normal observers, a measure of the strength of the depth percept (Cisarik & Harwerth, 2008; Doi, Tanabe, & Fujita, 2011; Henriksen, Cumming, & Read, 2016a; Henriksen, Read, & Cumming, 2016b; Julesz & Tyler, 1976; Tyler & Julesz, 1980). We were interested in providing a measure of the quality of binocular vision without disparity processing. In particular, we wanted to know the spatial dependence of our sensitivity to detect interocular correlation. Often, patients have fusion but no stereopsis. Thus one reason for asking this question is that, in amblyopes who lack or have deficient binocular vision without measurable stereopsis, there is a need to be able to assess the quality of binocular processing, both before and after treatment. An accurate measure of interocular correlation sensitivity and how it varies across space could quantify the degree of binocular function after fusion but before stereopsis.

Previous studies showed that the human visual system is indeed able to detect interocular correlation in the zero disparity case and that it depends to some extent on the contrast of the monocular signals (Cormack, Stevenson, & Schor, 1991; Julesz & Tyler, 1976; Stevenson, Cormack, Schor, & Tyler, 1992). Their stimuli were broadband in nature, being binary dots and they measured the detection of a level change in interocular correlation over the field of view. Kingdom and colleagues also looked at local mismatches between the two eyes that were still broadband (Jennings & Kingdom, 2016; Malkoc & Kingdom, 2012). We are interested in the spatial properties of our interocular correlation sensitivity and use bandpass textures whose interocular correlation is sinusoidally modulated at different "correlation frequencies." We define the interocular correlation (IOC) sensitivity function as the relationship between sensitivity for detecting correlation as a function of correlation spatial frequency. For the stimuli we constructed, when the modulation is null, a correlated and an uncorrelated pattern are uniformly blended in the two eye images resulting in a partially (50%) correlated stimulus over the whole area. Increasing the modulation parameter results in an increased correlation in the correlated

Citation: Reynaud, A., & Hess R.F. (2018). Interocular correlation sensitivity and its relationship with stereopsis. *Journal of Vision*, *18*(1):11, 1–11, https://doi.org/10.1167/18.1.11.

https://doi.org/10.1167/18.1.11 Received August 8, 2017; published January 23, 2018 ISSN 1534-7362

stripe and a decreased correlation in the "uncorrelated stripes" to reach, respectively, 100% and 0% correlation at maximum modulation, thereby making the stripes defined by the IOC difference clearly visible.

We see this as a potentially useful clinical measure for patients with deficient but not absent binocular function, and, in particular, in monitoring improvements from binocular treatment protocols. Here, we assess the role of contrast and the relationship between correlation sensitivity and disparity sensitivity as a function of spatial scale using a common protocol.

Methods

Observers

Six subjects (three males, including one author, average age = 28.2 ± 6.2 years, range: 18–36 years) participated in the main experiment. Thirty-four subjects (including the six previous ones, 19 males, average age = 26.7 ± 6.0 years, range: 18–40 years) participated in the population correlation study. All subjects had normal or corrected-to-normal visual acuity, normal stereopsis, and were free from ocular diseases. Informed consent was obtained from all subjects.

This research was approved by the Ethics Review Board of the McGill University Health Center. It was performed in accordance with the ethical standards laid down in the 1964 Declaration of Helsinki.

Interocular correlation and disparity sensitivity

Apparatus

Experiments were run on an Apple MacPro computer (Apple Inc., Cupertino, CA), with a Nvidia GeForce 8800 GT graphics card (Nvidia Corp., Santa Clara, CA), running on Linux Mint operating system (Linux Foundation, San Francisco, CA). Stimuli and experimental procedures were programmed with Matlab (MathWorks Inc., Natick, MA) using the Psychophysics (Brainard, 1997; Kleiner, Brainard, & Pelli, 2007; Pelli, 1997) and qCSF (Lesmes, Lu, Baek, & Albright, 2010) toolboxes.

Stimuli were displayed on a wide 3D-ready LED monitor (ViewSonic V3D231, 23 inches wide, 1920x1080 pixels, 60 Hz, mean luminance 100 cd/m^{-2}, gamma corrected; ViewSonic International Corp., New Taipei City, Taiwan). The stereo image input was in top-down digital video interactive format and was displayed in interleaved line stereo mode: The left eye image was displayed in even scanlines and the right eye image was displayed in odd scanlines.

The subjects viewed the stimuli at a viewing distance of 70 cm, in a dimly lit room, with passive polarized 3D glasses so that the left image was only seen by the left eye and the right image by the right eye (crosstalk = 1%; Spiegel, Baldwin, & Hess, 2017). The polarized filters had the effect of reducing the luminance to about 40%.

Data was analyzed off-line using Matlab (MathWorks) using the qCSF (Lesmes et al., 2010) and Palamedes (Prins & Kingdom, 2009) toolboxes.

Stimuli

Two types of stimuli were used in this study: the interocular correlation (IOC) stimuli and the disparity stimuli. Both were based on a filtered fractal noise carrier pattern in which either the interocular correlation or disparity could be modulated. The two-dimensional fractal noise was generated by weighting the amplitude spectrum of a uniformly distributed noise by one over spatial frequency (1/f), filtered at spatial frequencies of 0.94, 1.31, 1.83, 2.54, 3.54, 4.93, 6.87, and 9.57 c/d, with one octave bandwidth. Stimulus visibility was equated by scaling the carrier contrasts to 10 times the contrast thresholds measured for each carrier spatial frequency in a normative dataset (Reynaud et al., 2014): respectively, 32%, 27%, 25%, 27%, 33%, 47%, 75%, and 100% (clipped) for each spatial frequency. Stimuli were presented in a Gaussian envelope of 15° diameter (2x sigma).

Interocular correlation stimuli: The IOC stimuli consisted of two dichoptic noise patterns modulated by a sinusoidal oblique envelope of correlation (45° or 135°). So, at the peak of the sinusoid, the two patterns were maximally correlated and at the trough they were minimally correlated, creating a visual effect of luster (Jennings & Kingdom, 2016). Each eye's image was composed of two blended spatially filtered 2D fractal noise carrier: One of them was common in the two eyes c_c and one was different c_l or c_r. Before blending, the two carriers were modulated by out-of-phase sinusoidal envelopes m_c and m_a at a frequency f_m ¼ time the frequency of the carrier, which blending parameter m could be varied between 0 and 1, characterizing the amount of interocular correlation in the correlated stripes [Figure 1a top row, equation (1)].

$$\begin{aligned} m_c(x) &= \frac{1}{2}(1 + m\sin(2\pi f_m x)) \\ m_a(x) &= \frac{1}{2}(1 - m\sin(2\pi f_m x)) \end{aligned} \quad (1)$$

The resulting images I_l and I_r presented to the left and right eye were generated by blending the modulated carrier that was common to the two eyes' images c_c to either carrier c_l or c_r, respectively [Figure 1a bottom rows, equation (2)].

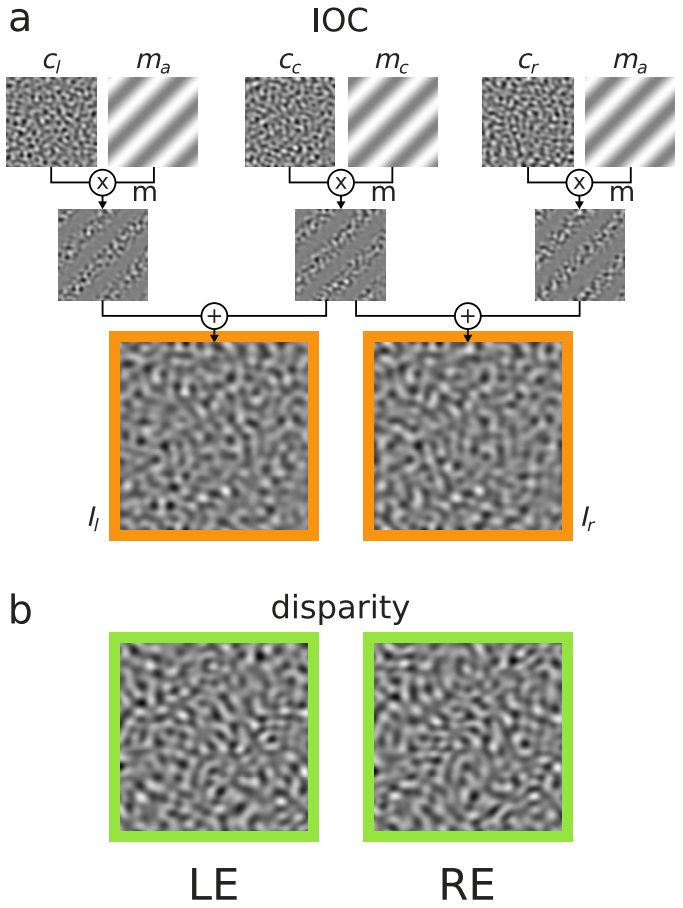

Figure 1. Stimuli. (a) Building of the interocular correlation (IOC) stimulus. The images viewed by the two eyes (bottom row) are composed of two blended filtered noise textures c_c and c_l or c_r respectively, modulated by out-of-phase sinusoidal envelopes m_c and m_a of 1/4 the frequency of the noise pattern. One of these textures is common in the two eyes c_c, constituting the correlated part of the stimulus. The modulation parameter m defines the amount of correlation present in the common stripes in the two eyes images I_l and I_r. (b) Disparity stimuli are constituted of similar filtered noise patterns, with horizontal disparity modulation defining oblique corrugation at 1/4 the frequency of the noise pattern (see Reynaud et al., 2015).

$$\begin{aligned} I_l &= c_c m_c + c_l m_a \\ I_r &= c_c m_c + c_r m_a \end{aligned} \quad (2)$$

At $m = 1$ the peaks of the sinusoidal envelope are correlated and the troughs uncorrelated, at $m = 0$, the pattern is 50% correlated over the whole image, thus the peaks and troughs of the envelope are no longer distinguishable.

Disparity stimuli: The disparity stimuli were stereograms similar to the ones used in Reynaud et al. (2015). They were composed with a spatially filtered 2D fractal noise carrier, as previously described. They presented oblique (45° or 135°) sinusoidal corrugations. The carrier frequency was four times the frequency of the corrugation (Figure 1b). Sinusoidal corrugation was introduced by shifting the carrier following a vertical sinusoid of opposite phase for each eye image. Non-integer pixel positions were linearly interpolated between neighboring pixels. Then, each pixel line was subsequently shifted one pixel to the right to obtain the 45° corrugation or to the left to obtain the 135° corrugation in each stereogram.

Procedures and analysis

A single-interval identification task was employed to estimate the sensitivity. The subjects' task was to identify the orientation of the correlation envelope or the disparity corrugation (45° or 135°). The trial time course was as follows: (a) a green fixation dot appeared on the screen, (b) the dot disappeared and the stimulus was presented for 1 s, unless indicated otherwise [see Julesz & Tyler (1976)] for an example of the temporal dependence for detection of full-field interocular correlation) (c) a red dot appeared to indicate to the subject that a response was needed, (d) the dot disappeared when the subject answered. Dot luminance was matched to that of the background, and no feedback was provided.

Constant stimuli: In a control experiment, the interocular correlation thresholds were measured individually with the Method of Constant Stimuli (MCS) for each spatial frequency: 0.24, 0.33, 0.46, 0.64, 0.89, 1.23, 1.72, and 2.39 c/d. The order in which participants performed the different spatial frequency conditions was randomized. The levels of modulation used were 0.10, 0.13, 0.16, 0.20, 0.25, 0.32, 0.40, 0.50, 0.64, 0.80, and 1.00. There were 20 repetitions per condition for each subject. Each measurement took approximately 15 minutes. The detection thresholds were then determined by fitting a Weibull function of the log-modulation $\bar{m}$ to the psychometric datasets [equation (3)].

$$F_W(\bar{m}; \alpha, \beta) = 0.5 + 0.5 \times \left(1 - e^{-(\bar{m}/\alpha)^\beta}\right) \quad (3)$$

where α is the log-threshold and β the slope of the psychometric function. In case the psychometric function did not reach saturation, the threshold was set to 1. The standard deviation of the fitted parameters was estimated by a bootstrapping procedure.

Quick Sensitivity Functions: In the main experiment, to enable a relatively rapid measurement of the full IOC sensitivity function, we adapted the quick contrast sensitivity function (*qCSF*) method (Hou et al., 2010; Lesmes et al., 2010). The frequency range was truncated from 0.24 to 2.39 c/d. The initial gain prior was set to 10, the peak frequency prior was set to 0.5 c/d ,and the bandwidth prior was set to three octaves. To measure the disparity sensitivity, we used a comparable

version of the *qCSF*, the quick Disparity Sensitivity Function that we had previously adapted (*qDSF*; Reynaud, Gao, & Hess, 2015).

These methods estimate the log-sensitivity function S with the truncated log-parabola model [equation (4), Ahumada & Peterson; 1992, Lesmes et al., 2010, Watson & Ahumada, 2005]. The truncated log-parabola is described by four parameters: the peak gain γ_{max}, the peak frequency, f_{max}, the bandwidth β, and the truncation δ.

$$\begin{aligned} &S'(f) = \log_{10}(\gamma_{\max}) - \kappa\left(\frac{\log_{10}(f) - \log_{10}(f_{\max})}{\beta'/2}\right)^2 \\ &\text{if } f < f_{\max} \quad \text{and} \quad S'(f) < \log_{10}(\gamma_{\max}) - \delta \\ &\text{then } S(f) = \log_{10}(\gamma_{\max}) - \delta \\ &\text{else } S(f) = S'(f) \end{aligned} \tag{4}$$

with $\kappa = \log_{10}(2)$ and $\beta' = \log_{10}(2\beta)$.

If the estimated peak frequency fell below the measurable range, we set the peak gain γ_{max}, to the maximum measured sensitivity and the peak frequency, f_{max}, to the lowest boundary, i.e., 0.24 c/d.

Interocular balance measure

Apparatus

The interocular balance was measured using an Oculus Rift SDK1 with a nominal field of view of 90° and a resolution in each eye of 800x640 pixels on a Sony VAIO laptop computer (Sony Corp., Tokyo, Japan). Stimuli and experimental procedures were programmed with Matlab (MathWorks) using the Psychophysics toolbox (Brainard, 1997; Kleiner, Brainard, & Pelli, 2007; Pelli, 1997).

Procedures and analysis

The procedure used to measure the interocular balance was similar to the simultaneous matching experiment described in Reynaud and Hess (2016). An alignment task was performed beforehand. Subjects had to align two vertical line segments: a green one seen by the left eye and a red one seen by the right eye on top of each other in the middle of the viewing area. The coordinates of the two segments were then used to present stimuli.

To measure the interocular balance, four Gabor patches of spatial frequency 0.28 c/d, in sine phase and sigma 2.82°, were dichoptically presented in a square arrangement with distance of 16.9° from center to center. A black frame was presented around them in both eyes to aid fusion. The top-right and bottom-left patches constituted the reference and were presented in the right eye, and the top-left and bottom-right patches constituted the target and were presented to the left eye. The reference patches were presented at 80% contrast and the subjects' task was to then adjust the perceived contrast of the target patches to match that of the reference patches by pressing the left and right arrow keys of the keyboard. The interocular balance was reported as the ratio between the reference contrast and the matched contrast or the inverse to be between 0 and 1.

Results

Measurement of interocular correlation sensitivity

It is not obvious that our visual system is able to detect instantaneous similarities and discrepancies between the two eye images (Jennings & Kingdom, 2016) when they do not form the basis of a disparity. Previous studies have demonstrated that this is the case for spatially broadband dots (Cormack et al., 1991; Stevenson et al., 1992). Our stimuli are bandpass and we are asking the same question but for stimuli of restricted spatial scale. So, a first step in our study was to show the sensitivity to interocular correlation for bandpass stimuli of different spatial scale. Figure 2 shows the measured psychometric functions for the identification of the orientation of oblique stripes defined by interocular correlation as a function of the modulation parameter, describing the amount of correlation in the correlated stripes, for one observer at eight spatial frequencies.

We can see that for all spatial frequencies the psychometric functions are monotonic and smooth as a function of the modulation, which confirms that the visual system is sensitive to the sinusoidal changes in interocular correlation of the pink noise pattern used here. The minimum thresholds are estimated by fitting a Weibull function.

The interocular correlation (IOC) sensitivities, the inverse of the thresholds measured with the Method of Constant Stimuli (MCS) from the six observers, are shown as a function of spatial frequency in Figure 3a (diamonds). They mostly display a low-pass or bandpass profile. The dashed curves represent five iterations of the quick measurement of the IOC sensitivity as a function of spatial frequency that we adapted from the *qCSF* (Lesmes et al., 2010). The five repetitions of the quick measurement, while being quite variable, do definitely fall in the same range as the thresholds estimated by the MCS.

The average sensitivities estimated with the quick method and the MCS for the six observers are presented in Figure 3b. We can see that, on average, the two methods give similar results at high spatial

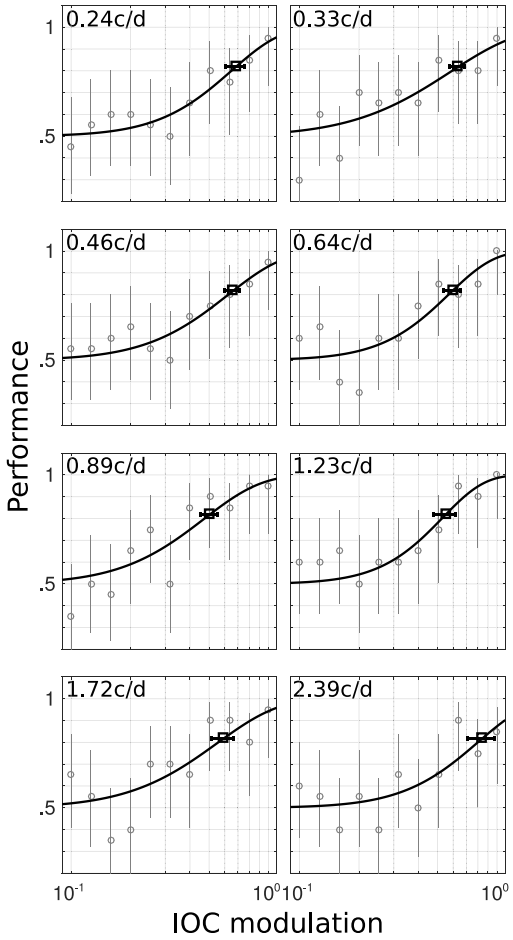

Figure 2. Psychometric functions of the IOC sensitivity obtained with the method of constant stimuli at each spatial frequency, respectively in each panel for one subject (S4). The data points (gray squares) represent the performance of the subject as a function of the envelope modulation. Thresholds (black squares) are estimated by fitting a Weibull function on the log-modulation (continuous line, Equation 3). Horizontal error bars represent *SD*.

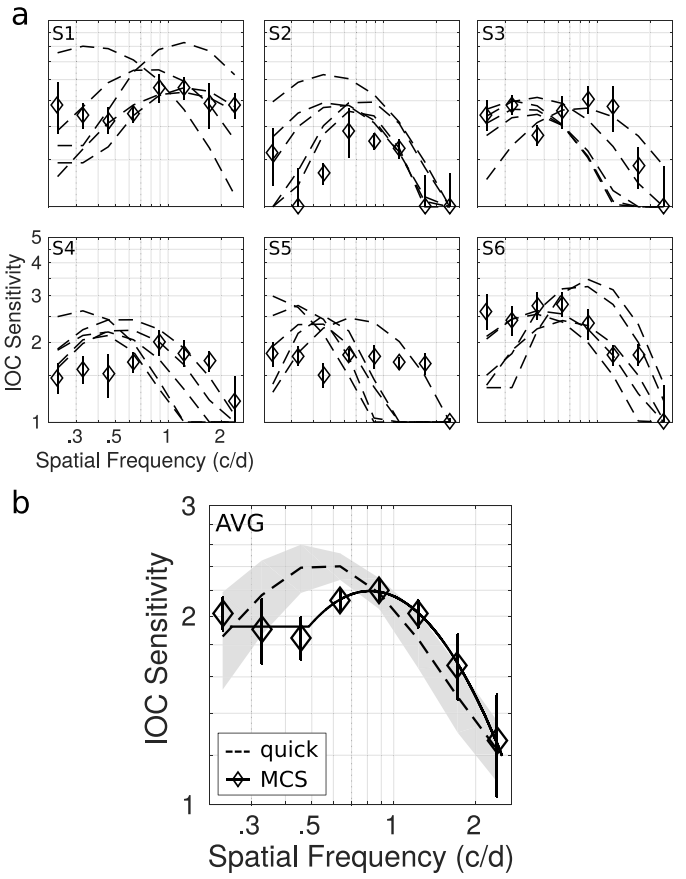

Figure 3. Comparison of the IOC sensitivity functions measured with the Method of Constant Stimuli (MCS) or with the quick method. (a) Six observers' individual data. Diamonds represent the sensitivity estimated with the MCS. Error bars represent standard deviation obtained with a bootstrap procedure. Dashed curves represent five repetitions of the quick method. (b) Average data for the six observers. Diamonds represent the average sensitivity estimated with the MCS; error bars are standard deviation. The dashed curve represents the average sensitivity measured with the quick method; the shaded area indicates the *SD*.

frequencies; however, the quick method gives slightly higher sensitivities at low spatial frequencies.

To better quantify the quality of these fits we wanted to know if the quick estimate for one observer is more strongly correlated with the MCS estimate obtained for that observer than it is for other observers. Thus, we computed the distance (as 1-norm, sum of absolute differences across spatial frequencies) between the two sensitivities obtained with the two measuring methods for each pair of subjects. Two subjects (S1 and S6) were best correlated with themselves. On average, the distance within a subject was 24% lower than the mean distance across all subjects. Therefore, the quick method is accurate enough and useful for comparative purposes. For example, we were able to compare this method and the *qDSF* previously adapted (Reynaud et al., 2015), to establish the relationship between IOC and disparity sensitivity functions for different stimulus durations and contrasts. Hence the rest of the data presented in this paper was obtained using the quick methods.

Influence of stimulus duration

The effect of time integration on the IOC and disparity sensitivity is shown in Figure 4 for the average IOC and disparity sensitivity functions over subjects in panels a and b, respectively. Stimulus durations were 0.05, 0.1, 0.15, 0.25, 0.5, 1, 2, and 3 s. We can directly see on these graphs that both sensitivities increase with longer exposure time, particularly at high frequencies.

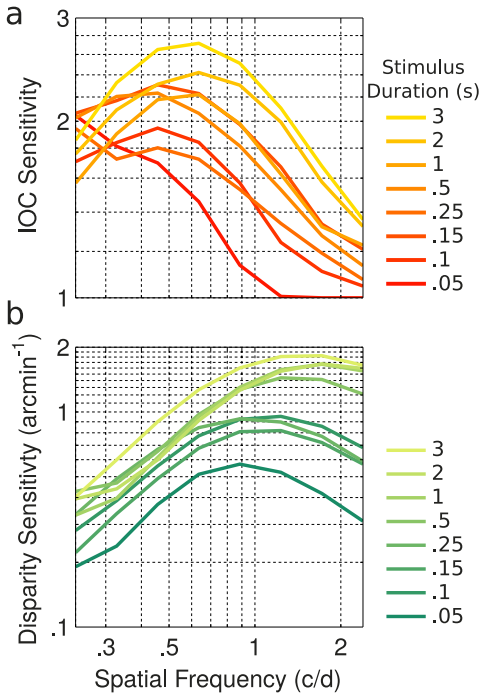

Figure 4. Effect of duration on the disparity and IOC sensitivity functions. (a) IOC sensitivity as a function of spatial frequency for stimulus durations ranging from 0.05 (red) to 3 s (yellow). (b) Disparity sensitivity as a function of spatial frequency for stimulus durations ranging from 0.05 (green) to 3 s (lime). Data averaged over six subjects.

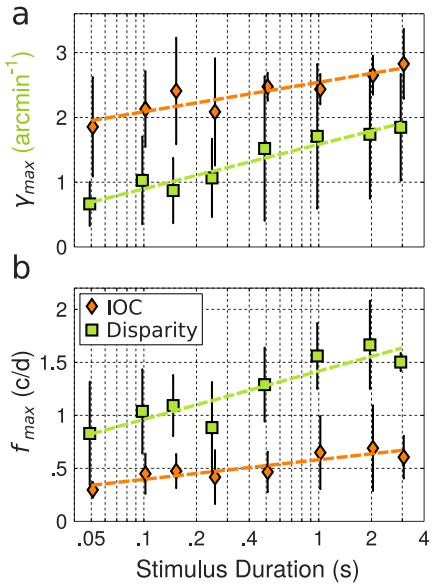

Figure 5. Evolution of the sensitivity functions parameters as a function of stimulus duration. (a) Gain as a function of stimulus duration for the IOC (orange diamonds) and disparity (green squares) sensitivity functions. The gain for the disparity sensitivity is expressed in arcmin^{-1}. (b) Peak frequency as a function of stimulus duration for the IOC (orange diamonds) and disparity (green squares) sensitivity functions. Error bars represent *SD* between subjects.

This is characterized by an increase in the gain and a shift toward higher frequencies.

This increase in gain and shift in tuning is quantified in Figure 5 where the maximum gain γ_{max} (Figure 5a) and peak frequency f_{max} (Figure 5b) of the IOC (diamonds) and disparity (squares) sensitivity functions are plotted as a function of the stimulus duration. It is apparent that the peak frequency and the maximum gain both increase as a function of the stimulus duration, showing a similar trend for the two sensitivities (Hess & Wilcox, 2006).

Influence of contrast

We now investigated the effect of a monocular or binocular contrast reduction on these two related sensitivities. The contrast was reduced to 0.3, 0.5, or 0.7 of the base contrast set for each spatial frequency (see Methods).

The average IOC sensitivity as a function of spatial frequency for various fractions (i.e., 0.3, 0.5, 0.7, and 1) of the base contrast is plotted for a binocular contrast reduction in Figure 6a and for a monocular contrast reduction in Figure 6b. For both viewing conditions, the sensitivity for 0.3 contrast is much reduced. In this case, the shape looks more bandpass for the binocular contrast reduction and more low pass for the monocular one. However, we think these tuning shapes are not really representative of the actual sensitivity and may be a consequence of a forced shape of the *qCSF* algorithm when the sensitivity is very low. The IOC sensitivity increases at higher contrast and overall the sensitivity seems to be slightly lower in the case of a binocular contrast reduction compared with a monocular one.

The disparity sensitivities for the same contrast conditions are plotted in Figure 6c for the binocular contrast reduction and Figure 6d for the monocular contrast reduction. Here again, the disparity sensitivity increases with contrast and seems to be slightly lower in the binocular contrast reduction condition. In other words, a binocular contrast reduction has a bigger impact on the IOC and disparity sensitivity than a monocular one, but this difference seems very small.

This monocular/binocular difference concerning the effect of contrast on stereopsis goes in the opposite direction to that of a number of previous studies that have used narrowband test stimuli at low spatial frequencies (Halpern & Blake, 1988; Legge & Yuanchao, 1989); however, it confirms the results of a number of other studies where spatially broadband stimuli—meaning containing high spatial frequencies—have been used (Cormack, Stevenson, & Landers, 1997; Hess, Liu, & Wang, 2003)

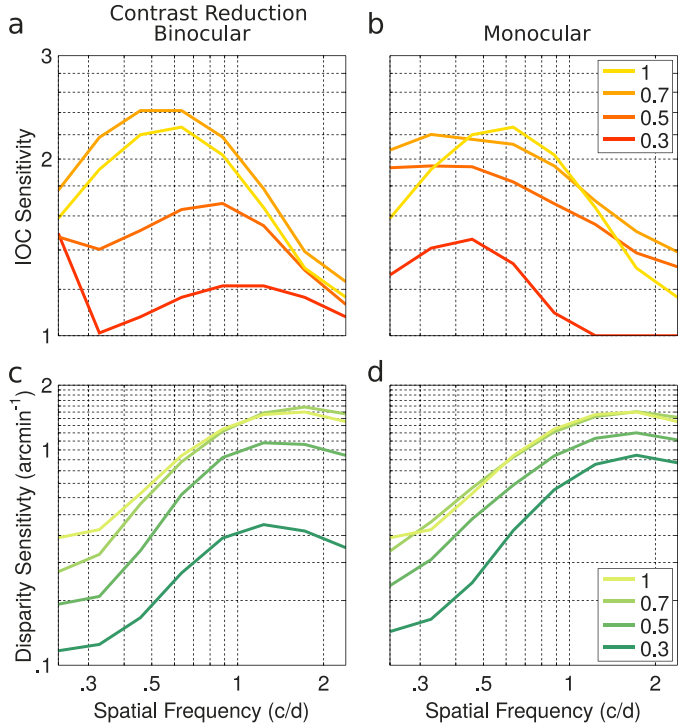

Figure 6. Effect of contrast on the disparity and IOC sensitivity functions. (a) IOC sensitivity as a function of spatial frequency for a binocular contrast ranging from 0.3 (red) to 1 (yellow), the maximum contrast set. (b) IOC sensitivity as a function of spatial frequency for a monocular contrast in the dominant eye ranging from 0.3 (red) to 1 (yellow), the maximum contrast set. The contrast in the non-dominance eye is always at maximum. (c) Disparity sensitivity as a function of spatial frequency for a binocular contrast ranging from 0.3 (green) to 1 (lime), the maximum contrast set. (d) Disparity sensitivity as a function of spatial frequency for a monocular contrast in the dominant eye ranging from 0.3 (green) to 1 (lime), the maximum contrast set. The contrast in the non-dominant eye is always at maximum. Data averaged over six subjects.

A quantitative assessment of the sensitivity function parameters is plotted in Figure 7. The values reported here look slightly different from that reported in Figure 6 because there is a difference between the average of the data and the average of the fit parameters. We can see clearly that the gain of the sensitivity functions increases with contrast for both IOC and disparity sensitivities, being apparently slightly higher for the monocular contrast reduction than for the binocular one (Figure 7a). However, for both disparity and IOC sensitivities, the peak frequency is comparable in both viewing conditions and increases very minimally with contrast. Indeed, it is only for the IOC sensitivity in the binocular contrast reduction condition that the slope of the regression of the peak frequency f_{max} on the log-axis is significantly positive ($p < 0.05$).

These observations suggest that a monocular or binocular contrast reduction only affects the gain of the

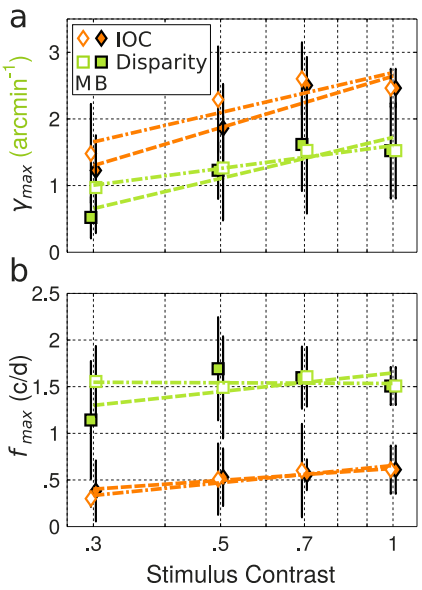

Figure 7. Evolution of the sensitivity functions parameters as a function of contrast. (a) Gain as a function of monocular contrast reduction (open symbols) or binocular contrast reduction (closed symbols) for the IOC (diamonds) and disparity (squares) sensitivity functions. The gain for the disparity sensitivity is expressed in arcmin-1. (b) Peak frequency as a function of monocular contrast reduction (open symbols) or binocular contrast reduction (closed symbols) for the IOC (orange diamonds) and disparity (green squares) sensitivity functions. Error bars represent *SD* between subjects.

disparity and IOC sensitivity functions without affecting their tuning. As they do with stimulus duration, these two sensitivities seem to share a similar contrast dependency.

Correlation in the population

To investigate further the dependency between these two sensitivities, we conducted a correlation study on a larger pool of observers. We measured the IOC (Figure 8a) and disparity (Figure 8b) sensitivity functions of 34 observers. There is a noticeable interindividual variability for the two sensitivities. However, although the disparity sensitivity could present low-pass, bandpass or high-pass profiles within the tested range (0.24–2.39 c/d) among individuals, it seems that no observer shows a high-pass tuning for IOC sensitivity. The mean, *SD*, and coefficient of variations of the sensitivity function maximum gain γ_{max} and peak frequency f_{max} population parameters are shown in Table 1. The lack of high-pass tuning for the IOC results in a significantly lower peak frequency f_{max} (Wilcoxon signed-rank test, $p < 10^{-6}$) and lower relative variance of the gain γ_{max} (indicated by the coefficient of variation c_v), compared to the disparity sensitivity (two-tailed F test on the log values of the maximum gain γ_{max}, $\alpha = 0.05$; Lewontin, 1966).

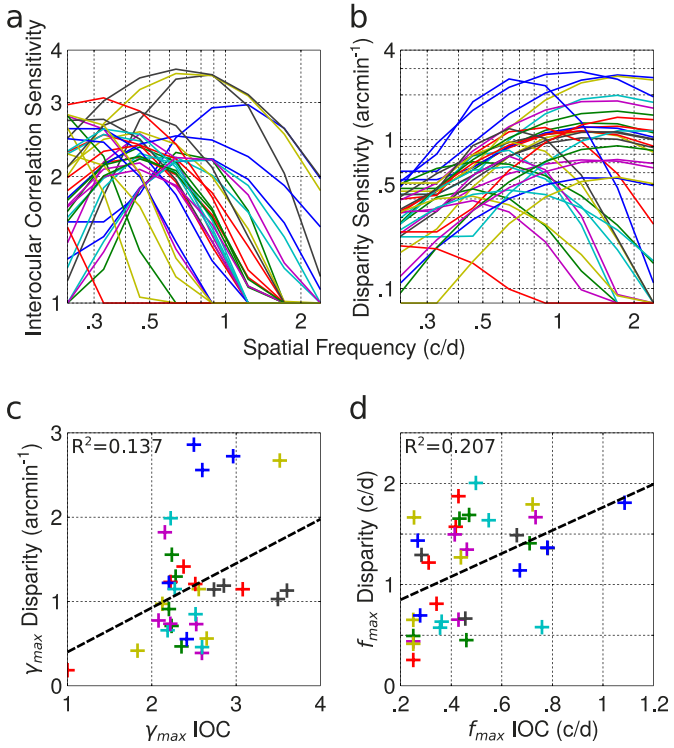

Figure 8. Population data of 34 individual observers. Colors are matched in the four panels. (a) Disparity sensitivity as a function of spatial frequency. (b) IOC sensitivity as a function of spatial frequency. (c) Correlation between the max gain γ_{max} for IOC (abscissa) and disparity (expressed in arcmin^{-1}, ordinates) sensitivities. (d) Correlation between the peak frequency f_{max} for IOC (abscissa) and disparity (ordinates) sensitivities

However, even if their tuning shapes are different, these two sensitivities seem to be fairly correlated. The Figure 8c scatterplot represents interindividual correlation between the maximum gain of the disparity and the IOC sensitivity functions ($R^2 = 0.137$). In Figure 8d, the correlation between the peak frequency of the disparity and the IOC sensitivity functions ($R^2 = 0.207$) is plotted. These two correlations are both positive and significant ($p < 0.05$). However, after a bootstrap analysis, the correlation between the gains is not significant anymore on average, meaning the correlation is mostly driven by the leftmost point in panel c.

	γ_{max}			f_{max}		
	μ	σ	cv	μ	σ	cv
IOC	2.47	0.49	0.20	0.47	0.21	0.44
Disparity	1.17	0.69	0.59	1.16	0.52	0.45

Table 1. Mean (μ), *SD* (σ), and coefficient of variation (cv) of the distributions of the estimates of the maximum gain γ_{max}, and the peak frequency f_{max}, for the IOC and disparity sensitivity functions. Frequencies are expressed in c/d. Disparity gain is expressed in arcmin^{-1}.

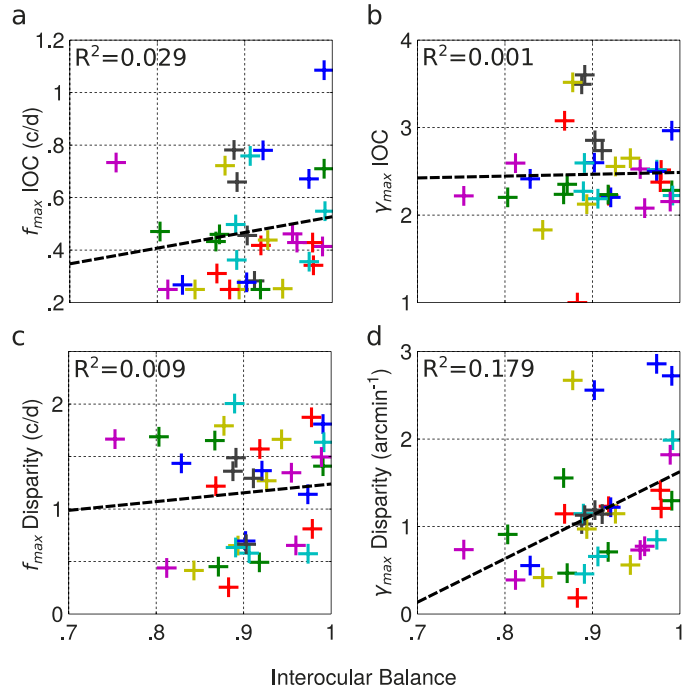

Figure 9. Correlation between interocular balance and binocular functions for the population of 34 observers. Correlation between interocular balance (abscissa) and (a) peak frequency f_{max} of the IOC sensitivity, (b) max gain γ_{max} of the IOC sensitivity, (c) peak frequency f_{max} of the disparity sensitivity, and (d) max gain γ_{max} of the disparity sensitivity.

These correlations suggest a link between the underlying mechanisms responsible for IOC and disparity. To assess if this could be because both of these sensitivities are dependent on a common lower-level factor, we looked at the correlation between these sensitivities and ocular dominance.

The interindividual correlations between the ocular dominance or interocular balance and the IOC sensitivity function's maximum gain and peak frequency parameters are represented as scatterplots in Figure 9a and b. These correlations are low and not significant. The correlation between the interocular balance and the peak frequency of the disparity sensitivity function is not significant either (Figure 9c). However, the correlation between the interocular balance and the gain of the disparity sensitivity function is positive and significant (Figure 9d), in accordance with the observations of Xu, He, & Ooi. (2011).

Discussion

We show that subjects can reliably detect the interocular correlation of bandpass elements, extending the conclusions of Cormack et al. (1991) who used broadband elements. By modulating the spatial distri-

bution of the interocular correlation, we define the interocular correlation spatial sensitivity function and show it has a bandpass or low-pass shape. Using the *qCSF* approach (Lesmes et al., 2010) we provide a convenient method of measurement that might be suitable in the clinic. This may provide a much-needed measure of the strength of binocular vision when fusion can be demonstrated but disparity processing is absent.

The use of the *qCSF* method is not without problems (Lesmes et al., 2010). In particular, the toolbox does not output the variance of the estimated parameters so it is not possible to know each subject's variability. Furthermore, it constrains the shape of the sensitivity function to be unimodal, which could generate artefactual profiles. Despite these limitations, the good accuracy of the estimations and the brevity of the approach allow one to collect a lot of data in a large sample of subjects.

An interesting issue is whether our sensitivity for interocular correlation per se is a good predictor of disparity sensitivity. We assessed the relationship between the sensitivities for interocular correlation and disparity as a function of spatial scale. We provided both duration and contrast data on the relationship between interocular correlation and disparity sensitivity. In terms of duration, both sensitivity functions show a similar dependence on duration (Hess & Wilcox, 2006): The gain is reduced and the position of peak is shifted to lower values for shorter durations. In terms of contrast, both interocular correlation sensitivity and disparity sensitivity show a greater dependence on binocular as opposed to monocular changes in contrast (Cormack et al., 1997; Hess et al., 2003). Also for contrast reduction, both functions show a change in gain but not peak position. By examining the intersubject variability for both IOC sensitivity and disparity sensitivity, there is a significant correlation for both the gain and peak position parameters. Despite this correlation between IOC sensitivity and disparity sensitivity across a number of different dimensions, the fact that the IOC frequency tuning cutoff is never as high as the disparity tuning cutoff would indicate that these two modalities are influenced by a common mechanism but that disparity processing may require an extra processing level. Interestingly, we recently observed (Reynaud & Hess, 2017) that in this spatial frequency range, disparity processing is mediated by two channels: a low and a high spatial frequency one; the low spatial frequency one showing similar tuning as the IOC sensitivity. Therefore, we speculate that this low spatial frequency channel could be common to the two mechanisms whereas the high spatial frequency one could be specific to disparity processing.

We also observed a correlation between the interocular balance and the amplitude of the disparity sensitivity function (Figure 9d), which means that the more balanced the two eyes are, the better the stereo sensitivity (Xu et al., 2011). This has to be put in perspective with the fact that we do observe a reduction in IOC and disparity sensitivity when contrast is reduced (Cormack et al., 1991). However, this reduction is worse when the contrast is reduced binocularly compared to monocularly. This observation suggests that the binocular visual system is computing an operation-like cross-correlation without normalization between the two eye images. This operation could be implemented by V1 neurons (Read & Cumming, 2007; see review in Read & Cumming, 2017), which indeed do increase their firing rate with contrast (Albrecht & Hamilton, 1982), confirming this operation is not normalized out. This would indicate that the IOC and disparity sensitivities mainly depend on the energy in the stimulus.

It is our hope that this new measurement of the interocular correlation sensitivity function could help in better understanding the binocular deficiency in amblyopia and may provide a more sensitive method of monitoring improvements to binocular function other than the disparity processing stage for binocular therapies (Hess, Mansouri, & Thompson, 2010; Li et al., 2013; To et al., 2011)

Keywords: disparity sensitivity, qDSF, binocular vision, stereopsis, interocular correlation, IOC

Acknowledgments

The authors thank the participants for their time and Professor Jenny Read for her invaluable comments on the manuscript. This paper was supported by a Canadian Institutes of Health Research (228103), an ERA-NET NEURON (JTC 2015), and a FRQS Vision Health Research Network of Quebec networking grant to RFH.

Commercial relationships: none.
Corresponding author: Robert Hess.
Email: robert.hess@mcgill.ca.
Address: McGill Vision Research, Department of Ophthalmology, McGill University, Montreal, Canada.

References

Ahumada A. J., & Peterson, H. A. (1992). Luminance-model-based DCT quantization for color image compression. *Proceedings Volume 1666, Human Vision, Visual Processing, and Digital Display III*, *1666*, 365–374.

Albrecht, D. G., & Hamilton, D. B. (1982). Striate cortex of monkey and cat: Contrast response function. *Journal of Neurophysiology*, *48*, 217–237.

Brainard, D. H. (1997). The Psychophysics Toolbox. *Spatial Vision*, *10*, 433–436.

Cisarik, P. M., & Harwerth, R. S. (2008). The effects of interocular correlation and contrast on stereoscopic depth magnitude estimation. *Optometry and Vision Science*, *85*, 164–173.

Cormack, L. K., Stevenson, S. B., & Landers, D. D. (1997). Interactions of spatial frequency and unequal monocular contrasts in stereopsis. *Perception*, *26*, 1121–1136.

Cormack, L. K., Stevenson, S. B., & Schor, C. M. (1991). Interocular correlation, luminance contrast and cyclopean processing. *Vision Research*, *31*, 2195–2207.

Doi, T., Tanabe, S., & Fujita, I. (2011). Matching and correlation computations in stereoscopic depth perception *Journal of Vision*, *11*(3):1, doi:10.1167/11.3.1. [PubMed] [Article]

Halpern, D. L., & Blake, R. R. (1988). How contrast affects stereoacuity. *Perception*, *17*, 483–495.

Henriksen, S., Cumming, B. G., & Read, J. C. A. (2016a). A single mechanism can account for human perception of depth in mixed correlation random dot stereograms. *PLoS Computational Biology*, *12*, e1004906.

Henriksen, S., Read, J. C. A., & Cumming, B. G. (2016b). Neurons in striate cortex signal disparity in half-matched random-dot stereograms. *Journal of Neuroscience,* 2016, *36*, 8967–8976.

Hess, R. F., Liu, C. H., & Wang, Y.-Z. (2003). Differential binocular input and local stereopsis *Vision Research*, *43*, 2303–2313.

Hess, R. F., Mansouri, B., & Thompson, B. (2010). A new binocular approach to the treatment of amblyopia in adults well beyond the critical period of visual development. *Restorative Neurology and Neuroscience*, *28*, 793–802.

Hess, R. F., & Wilcox, L. M. (2006). Stereo dynamics are not scale-dependent. *Vision Research*, *46*, 1911–1923.

Hou, F., Huang, C.-B., Lesmes, L., Feng, L.-X., Tao, L., Zhou, Y.-F., & Lu, Z.-L. (2010). qCSF in clinical application: Efficient characterization and classification of contrast sensitivity functions in amblyopia. *Investigative Ophthalmology and Vision Science*, *51*, 5365–5377. [PubMed] [Article]

Jennings, B. J., & Kingdom, F. A. A. (2016). Detection of between-eye differences in color: Interactions with luminance. *Journal of Vision*, *16*(3):23, doi:10.1167/16.3.23. [PubMed] [Article]

Julesz, B., & Tyler, C. W. (1976). Neurontropy, an entropy-like measure of neural correlation, in binocular fusion and rivalry *Biological Cybernetics*, *23*, 25–32.

Kingdom, F. (2012). Binocular vision: The eyes add and subtract. *Current Biology*, *22*, R22–R24.

Kleiner, M., Brainard, D., & Pelli, D. (2007). What's new in Psychtoolbox-3? Perception 36 ECVP.

Legge, G. E., & Yuanchao, G. (1989). Stereopsis and contrast. *Vision Research*, *29*, 989–1004.

Lesmes, L. A., Lu, Z.-L., Baek, J., & Albright, T. D. (2010). Bayesian adaptive estimation of the contrast sensitivity function: The quick CSF method. *Journal of Vision, 10*(3):17, 1–21. [PubMed] [Article]

Lewontin, R. C. (1966). On the measurement of relative variability. *Systematic Zoology*, *15*, 141–142.

Li, Z., & Atick, J. J. (1994). Efficient stereo coding in the multiscale representation. *Network: Computation in Neural Systems*, *5*(2), 157–174.

Li, J., Thompson, B., Deng, D., Chan, L. Y. L., Yu, M., & Hess, R. F. (2013). Dichoptic training enables the adult amblyopic brain to learn. *Current Biology*, *23*, R308–R309.

Malkoc, G., & Kingdom, F. A. (2012). Dichoptic difference thresholds for chromatic stimuli *Vision Research*, *62*, 75–83.

May, K., Zhaoping, L., & Hibbard, P. (2012). Perceived direction of motion determined by adaptation to static binocular images. *Current Biology*, *22*(1), 28–32.

Pelli, D. G. (1997). The VideoToolbox software for visual psychophysics: transforming numbers into movies. *Spatial Vision*, *10*(4), 437–442.

Prins, N., & Kingdom, F. A. A. (2009). *Palamedes: Matlab routines for analyzing psychophysical data*. Retrieved from http://www.palamedestoolbox.org/

Read, J. C. A., & Cumming, B. G. (2007). Sensors for impossible stimuli may solve the stereo correspondence problem. *Nature Neuroscience*, *10*, 1322–1328.

Read, J. C. A., & Cumming, B. G. (2017). Visual perception: Neural networks for stereopsis. *Current Biology*, *27*, R594–R596.

Reynaud, A., Gao, Y., & Hess, R. F. (2015). A normative dataset on human global stereopsis using the quick Disparity Sensitivity Function (qDSF). *Vision Research*, *113*(Pt A), 97–103.

Reynaud, A., & Hess, R. F. (2016). Is suppression just

normal dichoptic masking? Suprathreshold considerations. *Investigative Ophthalmology and Vision Science*, *57*(13), 5107–5115. [PubMed] [Article]

Reynaud A., & Hess R.F. (2017). Characterization of spatial frequency channels underlying disparity sensitivity by factor analysis of population data. *Frontiers in Computational Neuroscience*, *11*: 63.

Spiegel, D. P., Baldwin, A. S., & Hess, R. F. (2017). Ocular dominance plasticity: Inhibitory interactions and contrast equivalence *Scientific Reports*, *7*, 39913.

Stevenson, S. B., Cormack, L. K., Schor, C. M., & Tyler, C. W. (1992). Disparity tuning in mechanisms of human stereopsis. *Vision Research*, *32*, 1685–1694.

To, L., Thompson, B., Blum, J. R., Maehara, G., Hess, R. F., & Cooperstock, J. R. (2011). A game platform for treatment of amblyopia. *IEEE Transactions on Neural Systems and Rehabilitation Engineering*, *19*, 280–289.

Tyler, C. W., & Julesz, B. (1980). On the depth of the cyclopean retina. *Experimental Brain Research*, *40*, 196–202.

Watson, A. B., & Ahumada, A. J. (2005). A standard model for foveal detection of spatial contrast. *Journal of Vision*, *5*(9):6, 717–740, doi:10.1167/5.9.6. [PubMed] [Article]

Xu, J. P., He, Z. J., & Ooi, T. L. (2011). A binocular perimetry study of the causes and implications of sensory eye dominance *Vision Research*, *51*(23-24), 2386–2397.